

The effect of the Basset history force on particle clustering in Homogeneous and Isotropic Turbulence

S. Olivieri,¹ F. Picano,^{2,3} G. Sardina,^{3,4,5} D. Iudicone,⁶ and L. Brandt³

¹*DICCA, University of Genova, Via Montallegro 1, 16145 Genova, Italy*

²*Department of Industrial Engineering, University of Padova, Via Venezia 1, 35131, Padova, Italy*

³*SeRC and Linné FLOW Centre, KTH Mechanics, SE-100 44 Stockholm, Sweden*

⁴*Department of Meteorology, SeRC (Swedish e-Science Research Centre), Stockholm University, 106 91 Stockholm, Sweden*

⁵*Facoltà di Ingegneria e Architettura, UKE Università Kore di Enna, Enna, 94100, Italy*

⁶*Stazione Zoologica A. Dohrn, villa Comunale, Naples, Italy*

(Dated: 14 September 2022)

We study the effect of the Basset history force on the dynamics of small particles transported in homogeneous and isotropic turbulence and show that this term, often neglected in previous numerical studies, affects the particle behavior even at high density ratios. The small-scale clustering typical of inertial particles is reduced when the Basset history term is considered. We examine the contribution of this force to the total particle acceleration and demonstrate that, on average, it is responsible for about 10% of the total acceleration and is particularly relevant during rare strong events.

Introduction. Turbulent flows with dispersed phases can be found in several engineering applications and natural phenomena. On one side, we may recall sprays of droplets¹ and solid particles², typical of many combustion systems, whereas rain formation³, sediment transport⁴ and plankton⁵ are examples of natural flows. Preferential concentration in specific flow events affects the sedimentation rate of heavy particles⁶ and the plankton dynamics in the ocean⁵. The collision rate^{7,8} among droplets in a turbulent cloud determines the accretion rate and consequently the time for rain formation. These and similar processes are still far to be fully understood⁹, even restricting the analysis to dilute dispersions of small particles. In these conditions, the transport properties depend on the particle inertia, or better the particle relaxation time τ_p , and on the particle to fluid density ratio R ¹⁰. Particles with high density ratio and relaxation time τ_p of the order of the flow dissipative time scale (Kolmogorov time) τ_η exhibit intense small-scale clustering¹⁰ increasing largely the probability to find a particle pair separated by distances below the typical dissipative flow length, η . The clustering is essentially induced by the compressibility of the particle velocity field due to the particle inertia¹⁰, as inertial particles cannot follow convoluted trajectories. The particle velocity field may also exhibit caustics, i.e. different particle velocities at the same position¹¹. Both these phenomena crucially influence the collision rate and make difficult to provide an accurate estimate of it.

The relevance of the forces determining the particle acceleration varies with the particle density ratio and size. The Lagrangian equation governing the motion of small particles dispersed in a flow has been formulated by Maxey and Riley¹², with some minor later modifications¹³. The particle acceleration is determined by the Stokes Drag, due to the viscous forces acting on the particle, the Pressure Gradient, related to the pressure difference on the opposite sides of the particle, the Added Mass, “additional mass” due to the accelerating surrounding fluid, Gravity and the Basset History force due to the unsteady diffusion of vorticity in the boundary layer around the particle. Armenio et al.¹⁴ numerically investigated the relevance of these different terms on particles dispersed in a turbulent channel flow. These authors found that the Pressure Gradient governs the particle dynamics for density ratios of order one, while the Stokes Drag is dominant at high density ratio ($R \sim 100$). They also reported that the Basset History term is not negligible with respect to the other forces for all cases explored. Nonetheless, they did not show significant differences on the particle dispersion in turbulent channel flows when including the Basset history force. Note however, that more complex phenomena, i.e. turbophoresis¹⁵, arise in wall-bounded flows due to the strong spatial inhomogeneity¹⁶. The large part of numerical studies on inertial particles do not account for the Basset History term, see Ref. 10 for a recent review, an approximation usually considered quite safe for particles with high density ratio R . In stratified turbulence the vertical dispersion of particles with $R \sim 1$ is found to be attenuated by about 15% – 20% when the Basset history term is considered in the dynamics¹⁷. Recently, Daitche and Tél¹⁸ have studied the effects of the Basset history term on particle transport in two-dimensional unsteady wakes and shown that the particle clustering and the caustic formation are strongly reduced when the history term is considered also for particles denser than the fluid. Similar observations are reported

also for particles advected in two-dimensional chaotic flows¹⁹. The main aim of the present work is to quantitatively characterize the effect of the Basset history term on particle clustering and its contribution to the instantaneous particle acceleration in three-dimensional homogenous and isotropic turbulence. We will show that the small-scale clustering of inertial particles is always reduced by the Basset history term even for density ratio $R = 1000$. In addition, we observe that the importance of the different terms determining the instantaneous particle acceleration change when the Basset history is considered.

Methodology. We will use an Eulerian-Lagrangian approach to describe the dynamics of the fluid and particle phases. The carrier flow is governed by the incompressible Navier-Stokes equations where we denote $\mathbf{u}(\mathbf{x}, t)$ the fluid velocity field, ρ_f the fluid density, and ν is the fluid kinematic viscosity. We consider rigid spheres smaller than the relevant hydrodynamic scales, i.e. the Kolmogorov length $\eta = (\nu^3/\epsilon)^{1/4}$ (with ϵ the average energy dissipation), and assume vanishing particle Reynolds number, $Re_p = r_p|V_0 - U_0|/\nu \ll 1$ with V_0 and U_0 the particle and fluid velocities, and r_p the particle radius. Dilute conditions are considered in order to neglect particle-particle interactions and the back-reaction on the carrier phase. Hence, the particle velocity obeys the Maxey-Riley equation¹²:

$$\frac{d\mathbf{V}}{dt} = \frac{\mathbf{u} - \mathbf{V}}{\tau_p} + \frac{\rho_f}{\rho_p} \frac{D\mathbf{u}}{Dt} + \left(1 - \frac{\rho_f}{\rho_p}\right)\mathbf{g} + \frac{1}{2} \frac{\rho_f}{\rho_p} \left(\frac{D\mathbf{u}}{Dt} - \frac{d\mathbf{V}}{dt}\right) + \sqrt{\frac{9}{2\pi} \frac{\rho_f}{\rho_p} \frac{1}{\tau_p}} \int_{-\infty}^t \frac{1}{\sqrt{t-\tau}} \frac{d}{d\tau}(\mathbf{u} - \mathbf{V}) d\tau \quad (1)$$

where $\mathbf{u}(\mathbf{X}(t), t)$ is the flow velocity sampled at the particle position, ρ_p is the particle density, $\tau_p = (2/9)(r_p^2/\nu)(\rho_p/\rho_f)$ is the particle response time and \mathbf{g} is the gravitational acceleration vector. The acceleration terms in the RHS of eq. (1) are the Stokes Drag, Pressure Gradient, Gravity, Added Mass and Basset History, respectively. The derivative form in the added mass term has been suggested by Auton *et al.*¹³. The particle position $\mathbf{X}(t)$ is given by $d\mathbf{X}/dt = \mathbf{V}(t)$.

Fixing the flow conditions, i.e. the Reynolds number, the particle dynamics depends only on three dimensionless parameters: the density ratio $R = \rho_p/\rho_f$, the Stokes number $St_K = \frac{\tau_p}{\tau_K}$, with $\tau_K = \nu/\eta$ the Kolmogorov time, and the Froude number $Fr = U/(g\tau_{ref})$ here approaching infinity (we neglect the gravitational force).

The Navier-Stokes equations are solved by means of Direct Numerical Simulations using a classic pseudospectral method on a triperiodic cubic domain, whereas particles are analyzed in a Lagrangian framework. A quadratic interpolation provides the values of flow quantities at the particle position, those needed to solve the Maxey-Riley equation. The particle velocity and trajectory are evolved in time by using a third-order Adams-Bashfort scheme.

The computation of the Basset history term, the integral term in the eq. (1), presents the greatest numerical challenge as it requires the full history of the particle acceleration. To evaluate this force at a reasonable cost, we use the method recently proposed in Ref. 20, briefly introduced here for completeness. The integration is split in two parts, denoted as window and tail. The first consists of a numerical integration over the interval $[t - t_{win}, t]$, considering N_w previous steps. The singularity of the kernel function $1/\sqrt{t-\tau}$ for $t = \tau$ is dealt with by the trapezoidal rule

$$\begin{aligned} \mathbf{F}_{Ba,win}(t) \approx & \frac{4}{3} C_{Ba} \sqrt{\Delta t} \mathbf{b}_0 + \sum_{n=1}^{N_w-1} \frac{4}{3} C_{Ba} \sqrt{\Delta t} \left[(n-1)\sqrt{n-1} - 2n\sqrt{n} + (n+1)\sqrt{n+1} \right] \mathbf{b}_n + \\ & + C_{Ba} \sqrt{\Delta t} \left[\frac{4}{3} (N_w - 1) \sqrt{N_w - 1} + \left(2 - \frac{4}{3} N_w\right) \sqrt{N_w} \right] \mathbf{b}_{N_w} \end{aligned} \quad (2)$$

where $C_{Ba} = 6r_p^2\rho_f\sqrt{\pi\nu}$, $\Delta t = t_{win}/N_w$ the time step and \mathbf{b}_n the discretized value of $\mathbf{b}(\tau) = \frac{d}{d\tau}(\mathbf{u} - \mathbf{V})$.

The remaining history $[-\infty, t - t_{win}]$ is approximated using recursive exponential functions leading to lower computational cost but still keeping high accuracy. As suggested in Ref. 20, we chose $N_w = 5$ for all the simulations as this value gives a good compromise between accuracy and computational effort.

All simulations were performed using 288³ grid points on a cubic domain of side $\mathcal{L} = 2\pi$. The turbulence is characterized only by the Taylor Reynolds number $Re_\lambda = u'\lambda/\nu \simeq 136$, based on the Taylor length $\lambda = \sqrt{\epsilon/(15\nu u'^2)}$ and the root-mean-square of the fluid velocity fluctuations u' .

We consider different combinations of density ratio R and Stokes number St_K : in particular at $R = 1$: $St_K = 0.01, 0.1$, at $R = 10$: $St_K = 0.01, 0.1, 1$, at $R = 1000$: $St_K = 0.01, 0.1, 1, 10$. $R = 1$ and $R = 10$ reproduce the behavior of small solid particles in liquids, while $R = 1000$ is typical of aerosol/droplets in gases. The Stokes numbers are selected to avoid particles larger than the hydrodynamic lengths, so within the limits of our model. For each parameter set, we performed simulations with and without the Basset

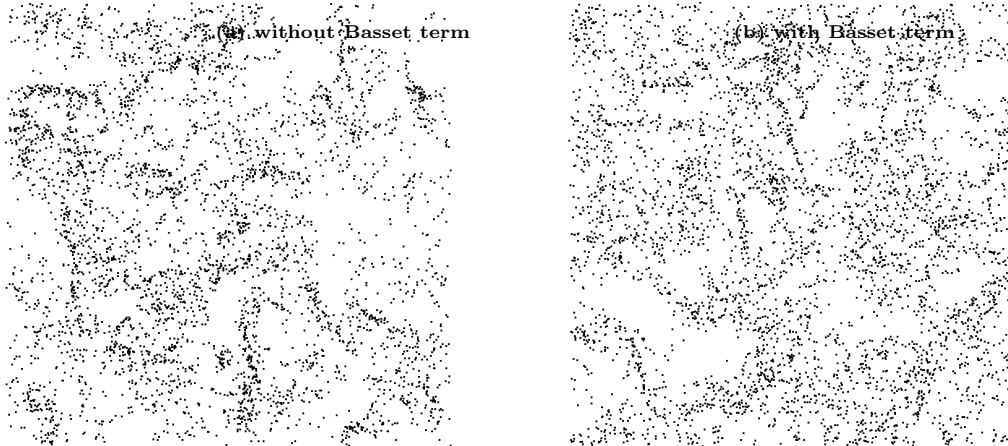


FIG. 1. Screenshots of particles distribution at $R = 10$, $St_K = 1$. (a) Results from a DNS without the Basset history term. (b) Results including all terms of eq. (1), thus also the Basset force.

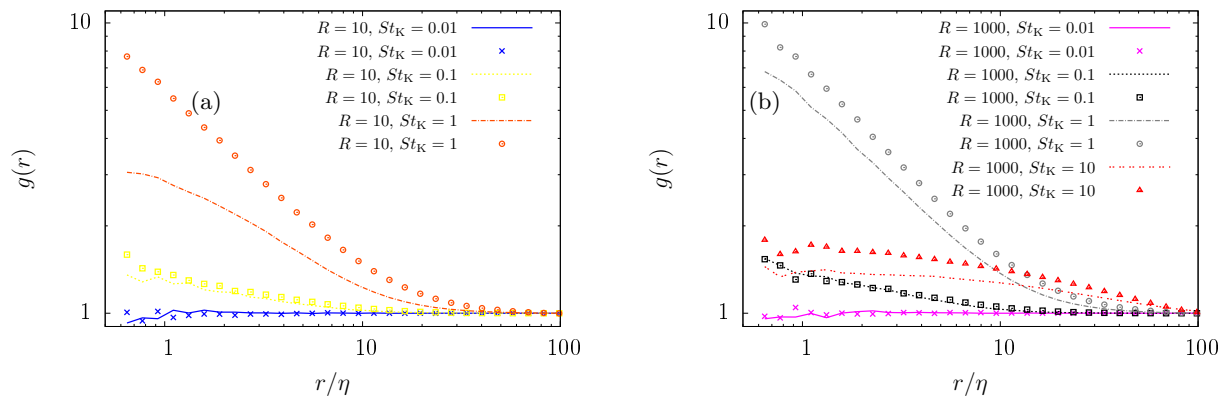


FIG. 2. The radial distribution function $g(r)$ versus particle distance r/η for (a) $R = 10$, and (b) $R = 1000$. Results including the Basset term are displayed by solid lines, results without Basset with symbols.

history force for comparison. We have simulated the unladen fluid phase until reaching the fully developed turbulent regime, when the particles are introduced with a random spatial distribution and the velocity of the fluid at the same position. We evolve the particle-fluid system for a time $T \simeq 700 \tau_K$ and save snapshots of particles quantities every $0.7 \tau_K$ time units in order to compute statistics.

Results Snapshots of the particle position from the simulation with $R = 10$ and $St_K = 1$ are displayed in figure 1. Results in (a) are obtained without the Basset history terms as often assumed in previous numerical studies on particle-laden turbulent flows. Small-scale clustering characterizes the particle distribution¹⁰: clusters and void regions large enough to be clearly appreciated at first sight. When the Basset history (BH) term is included, the particle segregation appears to be less intense, i.e. the Basset history term acts to smear out the clusters, as also recently observed in chaotic bi-dimensional flows^{18,19}. Interestingly this effect appears also for particles at high density ratios, i.e. $R = 1000$ (see below).

The clustering intensity can be quantified by the radial distribution function (RDF), $g(r)$, measuring the probability to find a particle pair at distance r normalized with that of a purely random Poissonian arrangement. The RDF for some of the most representative cases ($R = 10$ and $R = 1000$) is reported in Fig. 2 where we compare data obtained with (lines) and without (symbols) considering the BH. For both density ratios, we find the highest levels of small-scale clustering when $St_K = 1$, while the accumulation is weaker for the other Stokes numbers considered, in agreement with previous findings¹⁰. For all cases, the effect of the BH term is to weaken the clustering, confirming the visual impression given in figure 1.

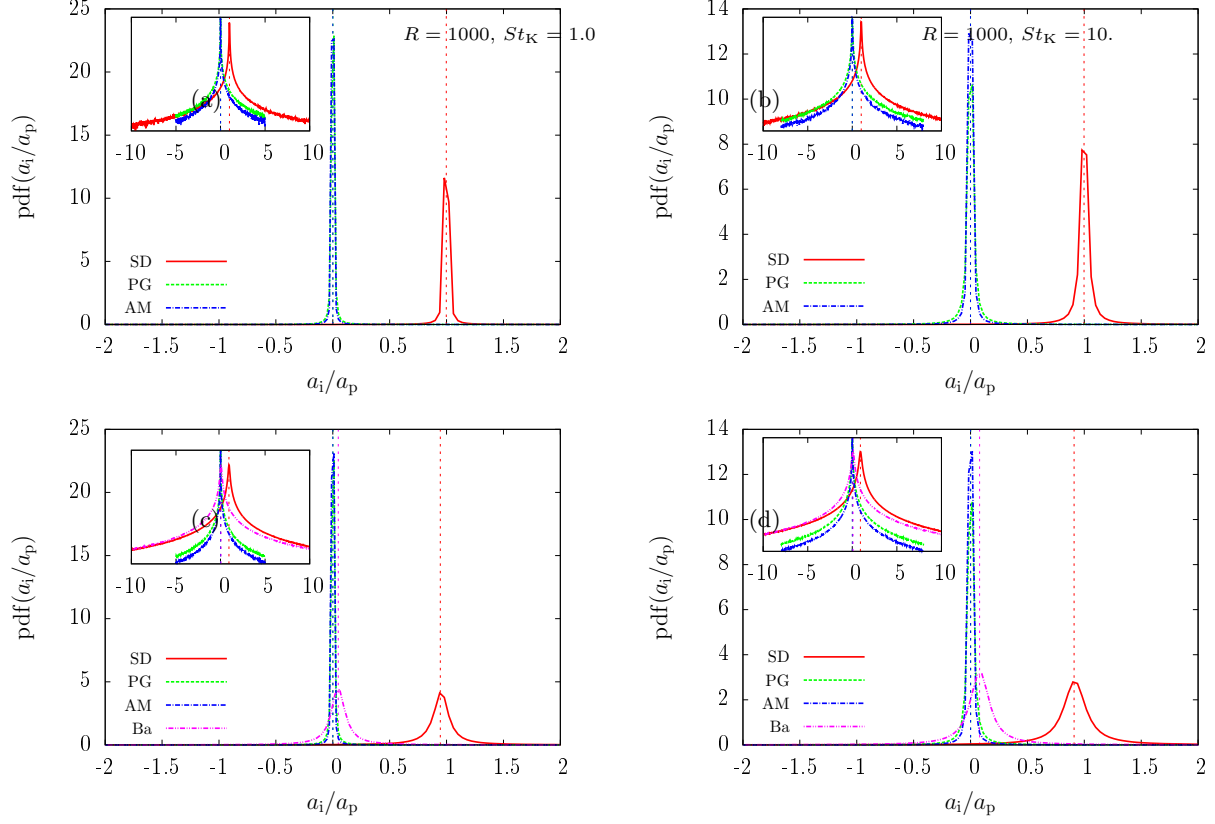


FIG. 3. P.d.f.'s of the acceleration a_i/a_p for particles with $R = 1000$ (heavy particles). Data from simulations without the Basset history term in (a) and (b); with the Basset term in (c) and (d).

Particles with $R = 1$ or tiny St_K do not show clustering, consistently with previous investigations²¹, and this does not change including the BH term.

The relative importance of the different forces appearing on the RHS of equation (1) is here studied by varying R and St_K . We aim to determine the relevance of the Basset history term to the total particle acceleration by comparing simulations with and without this term. Since the mean values of the whole acceleration is null in homogeneous and isotropic flows we will examine the p.d.f. (*probability density function*) of the different acceleration sources. In particular, we consider the p.d.f. of each term on the RHS of the Maxey-Riley equation (1) divided by the total particle acceleration,

$$1 = \frac{a_{SD}}{a_p} + \frac{a_{PG}}{a_p} + \frac{a_{Gr}}{a_p} + \frac{a_{AM}}{a_p} + \frac{a_{Ba}}{a_p} \quad (3)$$

where $a_p = dV/dt$ and the other terms denote vector components and not the modulus. By computing the p.d.f. of each of the quantities appearing above, a clear indication of the dominant contributions will be determined. Values around 1 will indicate a component that alone determines the overall instantaneous particle acceleration.

Fig. 3 reports the p.d.f.'s of the ratio a_i/a_p for the cases with the highest density ratio here investigated, $R = 1000$, and different Stokes numbers $St_K = 1 \div 10$. The figure 3(a) and (b) report simulations without BH and show that the Stokes Drag (SD) present a narrow distribution whose average lies around 1, while the distribution of the Pressure Gradient (PG) and the Added Mass (AM) both could be approximated by Dirac-delta functions centered on 0. In other words, the SD is the leading term driving the particle acceleration, in agreement with the usual assumptions in literature^{10,14}. The Basset force, however, does have an impact on the inertial particle dynamics as displayed in the bottom panels. Its presence widens the p.d.f. of the SD, and more importantly, moves its average to a value of about 0.9 (vertical lines in the figure). Even at this high density ratio, the BH influences the overall particle acceleration in an appreciable way. This explains the differences in the RDF's and clustering discussed above, see figure 2. In addition,

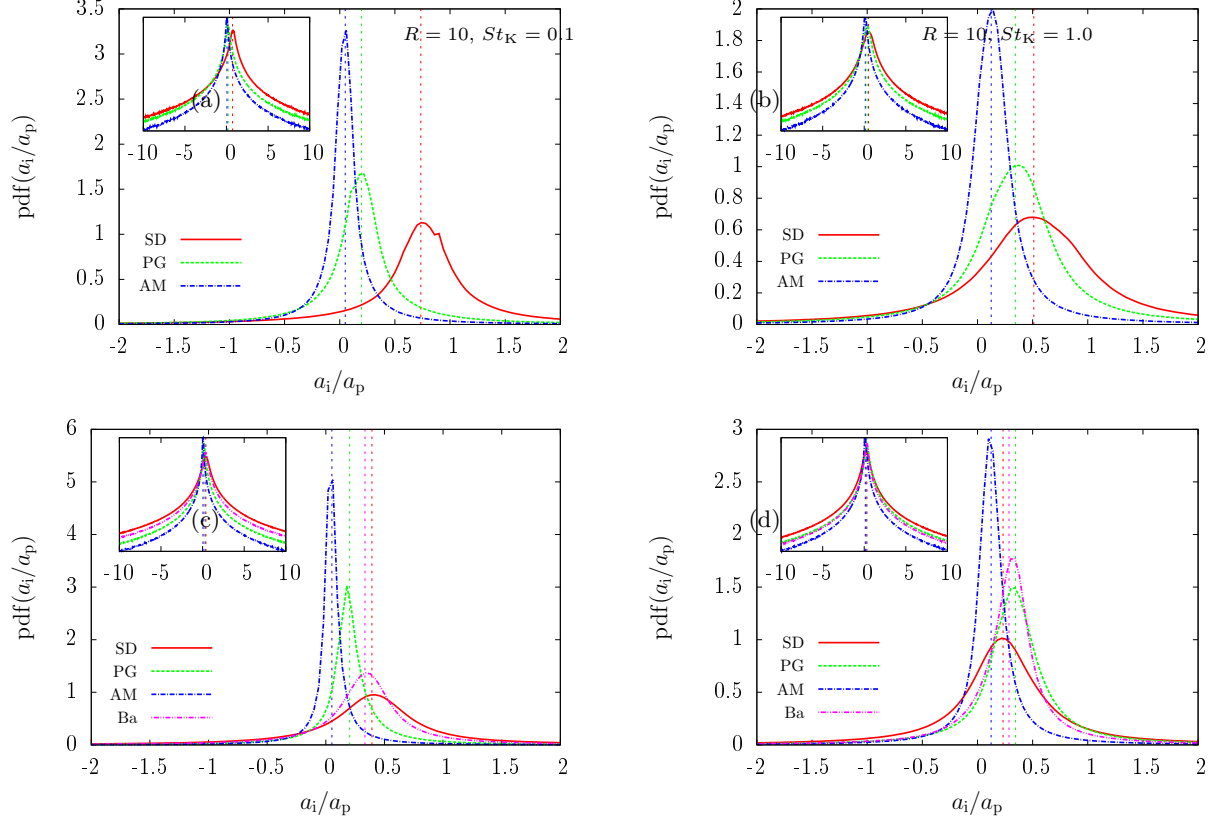


FIG. 4. P.d.f.'s of the acceleration a_i/a_p for particles with $R = 10$. Data from simulations without the Basset history term in (a) and (b); and with the Basset term in (c) and (d).

the lin-log plots in the insets reveal that both the SD and the BH exhibit long tails; rare intense events are even more influenced by the Basset history term. Particles with different Stokes number show a similar behavior (not reported here).

The behavior of particles with an intermediate density ratio, $R = 10$, is presented in Fig. 4. Unlike the case of particles with $R = 1000$, we do not find one dominant term, but the particle dynamics emerge from the contribution of the different forces, with significantly long tails. Examining the simulations where BH is not considered, figs. (a) and (b), we note that the PG becomes more and more important with respect to the SD when increasing the Stokes number. Most importantly, the impact of the BH is relevant for all Stokes numbers considered (see fig. c and d). Indeed, the average impact of the other terms, in particular SD, is strongly altered by the presence of the BH. The large difference in the clustering (RDF) shown by particles with $R = 10$ and $St_K = 1$ has to be ascribed to this change. Hence, at density ratios of the order $R \approx 10$, BH cannot be neglected to capture the correct particle dynamics.

Finally, we report some of the results for particles of density ratio $R = 1$. Although these particles do not show any clustering, it is interesting to document the strong alteration of the p.d.f.s of a_i/a_p when BH is taken into account especially at small Stokes numbers. We see in Fig. 5 that the leading term in the balance is the Stokes drag when BH is not considered, whereas it becomes the PG with the full model. Also for this case, we note the very long tails in the distribution of the SD.

Final remarks. The present work addresses the effect of the Basset history term (BH) on the dynamics of small particles dispersed in a turbulent homogenous isotropic flow. Different Stokes numbers $St_K = 0.01 - 10$ and density ratio $R = 1 - 1000$ have been considered. The BH is found to be relevant in the dynamics of particles with moderate density ratios, $R = 1$ and $R = 10$, where its presence alters the balance of the different terms that determine the particle acceleration. This has a relevant impact on the small-scale clustering observed at $R = 10$.

Even more unexpected is the result on the impact of BH on the dynamics of particles with high density ratio, $R = 1000$. Also here, the clustering intensity is found to decrease for Stokes number in the range

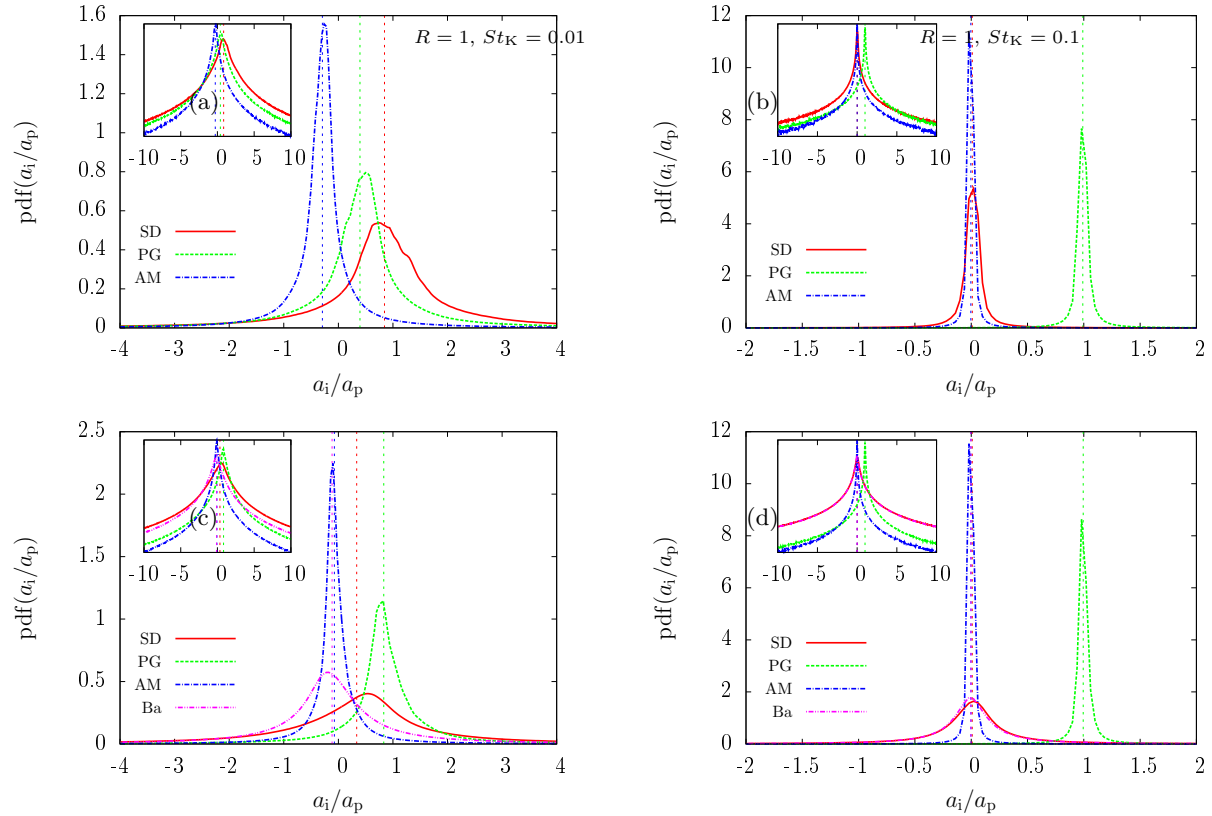


FIG. 5. P.d.f.'s of the acceleration a_i/a_p for particles with $R = 1$. Data from simulations without the Basset history term in (a) and (b); and with the Basset term in (c) and (d).

$St_K = 0.1 - 10$. Examining the p.d.f.'s of the terms determining the total particle acceleration, BH amounts to $\sim 10\%$ of the total. For the rest, the particle acceleration is determined by the Stokes Drag. It is also worth noting that the p.d.f.'s of the BH show long tails, meaning that this force is crucial for a correct representation of rare intense events of the particle dynamics. The effect of BH identified here could help to clarify some of the discrepancies between numerical and experimental results on particle dynamics that are still not fully understood, see e.g. Ref. 22. We believe that these findings will stimulate further investigations on dispersed particle transport where the Basset history term will need to be considered, and new modeling efforts based on comparison with detailed particle simulations as those recently appearing^{23–25}.

¹P. Domingo, L. Vervisch, and J. Réveillon, “Dns analysis of partially premixed combustion in spray and gaseous turbulent flame-bases stabilized in hot air,” *Combustion and Flame* **140**, 172–195 (2005).

²B A McDonald and S Menon, “Direct numerical simulation of solid propellant combustion in crossflow,” *J. Prop. and Power* **21**, 460–469 (2005).

³G Falkovich, A Fouxon, and MG Stepanov, “Acceleration of rain initiation by cloud turbulence,” *Nature* **419**, 151–154 (2002).

⁴L. O. Amoudry and A. J. Souza, “Deterministic coastal morphological and sediment transport modeling: A review and discussion,” *Rev. Geophysics* **49** (2011).

⁵C. S. Reynolds, *The Ecology of Phytoplankton*, Ecology, Biodiversity, and Conservation (Cambridge University Press, 2006).

⁶Lian-Ping Wang and Martin R Maxey, “Settling velocity and concentration distribution of heavy particles in homogeneous isotropic turbulence,” *J. Fluid Mech.* **256**, 27–27 (1993).

⁷R. A. Shaw, “Particle-turbulence interactions in atmospheric clouds,” *Annu. Rev. Fluid Mech.* **35**, 183–227 (2003).

⁸S. Sundaram and L. R. Collins, “Collision statistics in an isotropic particle-laden turbulent suspension. part 1. direct numerical simulations,” *J. Fluid Mech.* **335**, 109 (1997).

⁹W. W. Grabowski and L.-P. Wang, “Growth of cloud droplets in a turbulent environment,” *Annu. Rev. Fluid Mech.* **45**, 293–324 (2013).

¹⁰F. Toschi and E. Bodenschatz, “Lagrangian properties of particles in turbulence,” *Annu. Rev. Fluid Mech.* **41**, 375–404 (2009).

¹¹J. Bec, L. Biferale, M. Cencini, A. S. Lanotte, F. Toschi, *et al.*, “Intermittency in the velocity distribution of heavy particles in turbulence,” *J. Fluid Mech.* **646**, 527–536 (2010).

¹²M. R. Maxey and J. J. Riley, “Equation of motion for a small rigid sphere in a nonuniform flow,” *Phys. Fluids* **26**, 883–889 (1983), <http://link.aip.org/link/?PFL/26/883/1>.

- ¹³T. R. Auton, J. C. R. Hunt, and M. Prud'Homme, "The force exerted on a body in inviscid unsteady non-uniform rotational flow," *J. Fluid Mech.* **197**, 241–257 (1988).
- ¹⁴V. Armenio and V. Fiorotto, "The importance of the forces acting on particles in turbulent flows," *Phys. Fluids* **13**, 2437–2440 (2001).
- ¹⁵MW Reeks, "The transport of discrete particles in inhomogeneous turbulence," *J. Aerosol Sci.* **14**, 729–739 (1983).
- ¹⁶G. Sardina, P. Schlatter, L. Brandt, F. Picano, and C. M. Casciola, "Wall accumulation and spatial localization in particle-laden wall flows," *J. Fluid Mech.* **699**, 50–78 (2012).
- ¹⁷M. van Aartrijk and H. J. H. Clercx, "Vertical dispersion of light inertial particles in stably stratified turbulence: The influence of the basset force," *Phys. Fluids* **22**, 013301 (2010).
- ¹⁸A. Daitche and T. Tél, "Memory effects are relevant for chaotic advection of inertial particles," *Phys. Rev. Lett.* **107**, 244501 (2011).
- ¹⁹K. Guseva, U. Feudel, and T. Tél, "Influence of the history force on inertial particle advection: Gravitational effects and horizontal diffusion," *Phys. Rev. E* **88**, 042909 (Oct 2013).
- ²⁰M. A. T. van Hinsberg, J. H. M. Thije Boonkkamp, and H. J. H. Clercx, "An efficient, second order method for the approximation of the basset history force," *J. Comp. Phys.*, 1465–1478(2011).
- ²¹L. Fiabane, R. Zimmermann, R. Volk, J.-F. Pinton, and M. Bourgoïn, "Clustering of finite-size particles in turbulence," *Phys. Rev. E* **86**, 035301 (2012).
- ²²E Calzavarini, R Volk, M Bourgoïn, E Lévêque, J-F Pinton, and F Toschi, "Acceleration statistics of finite-sized particles in turbulent flow: the role of Faxén forces," *J. Fluid Mech.* **630**, 179 (2009).
- ²³F. Picano, W.-P. Breugem, D. Mitra, and L. Brandt, "Shear thickening in non-brownian suspensions: An excluded volume effect," *Phys. Rev. Lett.* **111**, 098302 (2013).
- ²⁴H. Homann, J. Bec, *et al.*, "Finite-size effects in the dynamics of neutrally buoyant particles in turbulent flow," *J. Fluid Mech.* **651**, 81 (2010).
- ²⁵A. G Kidanemariam, C. Chan-Braun, T. Doychev, and M. Uhlmann, "Direct numerical simulation of horizontal open channel flow with finite-size, heavy particles at low solid volume fraction," *New J. Phys.* **15**, 025031 (2013).